Astron. Astrophys. 344, 450–458 (1999)

ASTRONOMY AND ASTROPHYSICS

Interacting star clusters in the Large Magellanic Cloud⋆

Overmerging problem solved by cluster group formation

Stéphane Leon[1,2], **Gilles Bergond**[2,3], **and Antonella Vallenari**[4]

[1] DEMIRM, Observatoire de Paris, 61, Avenue de l'Observatoire, F-75014 Paris, France
[2] CAI-MAMA, Observatoire de Paris, 61, Avenue de l'Observatoire, F-75014 Paris, France
[3] DASGAL, Observatoire de Paris-Meudon, 5, Place J. Janssen, F-92195 Meudon, France
[4] Astronomical Observatory of Padova, Vicolo dell'Osservatorio 5, I-35122 Padova, Italy

Received 15 October 1998 / Accepted 15 December 1998

Abstract. We present the tidal tail distributions of a sample of candidate binary clusters located in the bar of the Large Magellanic Cloud (LMC). One isolated cluster, SL 268, is presented in order to study the effect of the LMC tidal field. All the candidate binary clusters show tidal tails, confirming that the pairs are formed by physically linked objects. The stellar mass in the tails covers a large range, from 1.8×10^3 to $3 \times 10^4 M_\odot$. We derive a total mass estimate for SL 268 and SL 356. At large radii, the projected density profiles of SL 268 and SL 356 fall off as $r^{-\gamma}$, with $\gamma = 2.27$ and $\gamma = 3.44$, respectively. Out of 4 pairs or multiple systems, 2 are older than the theoretical survival time of binary clusters (going from a few 10^6 years to 10^8 years). A pair shows too large age difference between the components to be consistent with classical theoretical models of binary cluster formation (Fujimoto & Kumai 1997). We refer to this as the "overmerging" problem. A different scenario is proposed: the formation proceeds in large molecular complexes giving birth to groups of clusters over a few 10^7 years. In these groups the expected cluster encounter rate is larger, and tidal capture has higher probability. Cluster pairs are not born together through the splitting of the parent cloud, but formed later by tidal capture. For 3 pairs, we tentatively identify the star cluster group (SCG) memberships. The SCG formation, through the recent cluster starburst triggered by the LMC-SMC encounter, in contrast with the quiescent open cluster formation in the Milky Way can be an explanation to the paucity of binary clusters observed in our Galaxy.

Key words: stars: formation – stars: Hertzsprung–Russel (HR) and C-M diagrams – galaxies: Magellanic Clouds – galaxies: star clusters – galaxies: stellar content

1. Introduction

The LMC possesses a large population of candidate binary clusters, having no counterpart in the Milky Way where only a few open clusters are known to be binary, as h&χ Persei (Subramiam et al.1995). In the LMC the existence of binary clusters was disclosed a decade ago (Bhatia & Hatzidimitriou 1988; Bhatia et al.1991). Using statistical arguments, Bhatia & Hatzidimitriou (1988) claimed that a considerable fraction of the suspected binary clusters must be physically linked.

However, on theoretical ground, their physical status and their properties (formation process, survival time, ...) remain unclear. De Oliveira et al.(1998) have performed N-body simulations of star cluster encounters explaining the presence of some morphological effects found in LMC cluster pairs as expanded halo, isophotal deformation and isophotal twisting. Fujimoto & Kumai (1997) have explained the formation of pairs in terms of oblique cloud-cloud collisions. As a result of these collisions, the clouds are split in two parts, forming the cluster pair. As a consequence, the two clusters have the same age. The lifetime of a proto-cluster is unknown, but is is estimated to be of 10^8 yr at maximum. This is the expected age difference between the two components of cluster pairs.

Clearly, this model runs into problems to account for the presence of non-coeval pairs of clusters as observed in the LMC (see Vallenari et al.1998). It has been proposed (Grondin et al.1992; Vallenari et al.1998) that the recent cluster burst formation some 10^8 yr ago could have been triggered by the interaction between the SMC and the LMC. Recent works on Galactic clusters (Grillmair et al.1995, hereafter G95; Leon et al.1999; Bergond et al.1999) have shown that the globular and open clusters disclose huge tidal tail extensions due to their interactions with the strong gravitational tidal field. In this framework, the study of the isolated and binary clusters in the LMC is interesting as probe of the star cluster shaping by the LMC tidal field. Moreover the LMC star clusters are found to have higher ellipticity than their galactic counterparts. Goodwin (1997) has suggested that tidal field of the parent galaxy is the dominant factor in determining ellipticity of the globular cluster. However high ellipticity can as well be the result of a different process: Sugimoto & Makino (1989) suggested that some of the most elliptical objects could be the rotating remnants of cluster mergers. They propose a scenario where some of the young clusters born in pairs from the proto-cluster gas, will eventually merge

Send offprint requests to: S. Leon (sleon@mesunb.obspm.fr)

⋆ Based on observations collected at the European Southern Observatory, La Silla, Chile

Table 1. Observed cluster properties: X and Y are the positions inside the LMC from Bica et al.(1996). The age is from Vallenari et al.(1998), except for NGC 1850 which is from Fischer et al.(1993). The diameter is from Bica et al.(1996) and the separation is from Bhatia et al.(1991).

Cluster	X (°)	Y (°)	Age (Log(yr))	Diam. (pc)	Sepa. (pc)
SL 268	+1.04	−0.11	8.65	12	
NGC 1850	+1.11	+0.70	7.95	12	
SL 349	+0.62	+0.40	8.70	12	19
SL 353	+0.66	+0.38	8.70	12	19
SL 356	+0.32	+0.14	7.85	15	39
SL 357	+0.34	+0.14	8.78	9	39
SL 385	+0.37	+0.16	8.18	10	10
SL 387	+0.44	+0.14	8.70	10	10

or be disrupted in a few 10^7 years. Stellar halo truncation by the tidal interactions and dynamical friction is decreasing progressively the ellipticity of the merger clusters. This paper discusses the properties of a sample of suspected binary clusters and the implications on the formation scenario.

The observations and the data reduction are presented in Sect. 2 and Sect. 3, respectively. The properties of individual cluster pairs are discussed in Sect. 4 and finally the conclusions are drawn in Sect. 5.

2. Observations and presentation of the cluster sample

The observations have been made in La Silla on December 16th-17th 1995, using the NTT ESO telescope equipped with EMMI and the ESO CCD #36 (0.27″/pixel). More details about the observations can be found in Vallenari et al.(1998) for all the clusters, except for NGC 1850. This cluster has been observed with the ESO 2.2 meter telescope in La Silla (0.46″/pixel). The observations of NGC 1850 are described in Vallenari et al. (1994).

The stellar photometry has been performed using DAOPHOT II and a conversion to the standard Johnson V and I has been done from calibration stars in the Landolt list. In Table 1 we present the cluster sample located in the west side part of the LMC bar: 6 are components of suspected binary systems (SL 349-SL 353, SL 356-SL 357, SL 385-SL 387). NGC 1850 can be considered as a binary or even triple system (Fischer et al.1993; Vallenari et al. 1994). SL 268 is an isolated object included to have a control cluster relative to the LMC gravitational tidal field.

3. Data reduction

3.1. Tidal tail extension

From the Color-Magnitude Diagram (CMD) contrast between the cluster and the field, we construct a signal/noise function s-n in the Color-Magnitude Space (CMS) for each pair: details of the method are given in G95. In Fig. 1 the function s-n is presented for NGC 1850: its main sequence termination point,

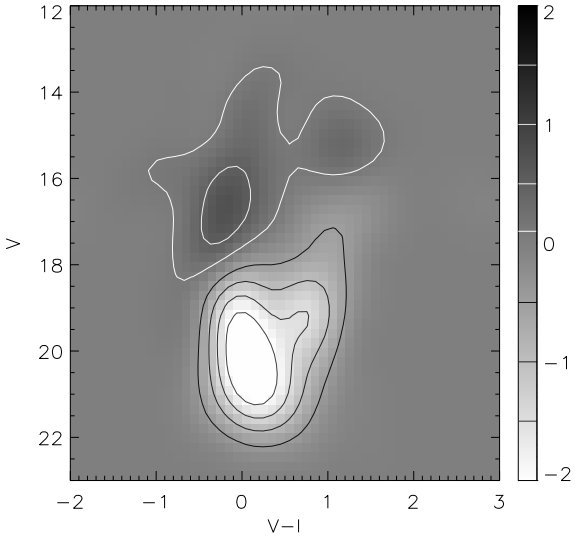

Fig. 1. Function s-n towards NGC 1850. A high s-n value in the color-magnitude space indicates a reliable separation for the underlying stars relative to the field stars.

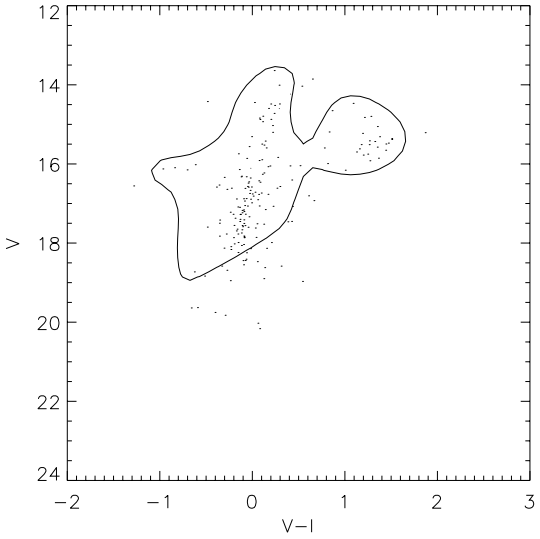

Fig. 2. CMD of the stars towards NGC 1850 and the contour which limits the area with a high S/N to select the stars.

because of its young age, is about $V \sim 16.5$ and the evolved star region is clearly seen with a good S/N. The low values of the function represent the main sequence stars of the LMC field population.

SL 349 and SL 353 are not distinguishable on the basis of their CMD, due to their similar age. We will treat both clusters as a whole to derive the tidal extension of the pair. SL 268 and SL 356 present the higher contrast relative to the field stars.In all the cases the highest S/N is for the upper part of the main sequence and for the evolved stars. From this s-n function, we select a high-S/N region in the CMS to filter the star catalog, as shown for NGC 1850 in Fig. 2. We present in Fig. 3 the areas in the CMS retained to select the stars for the whole sample of clusters.

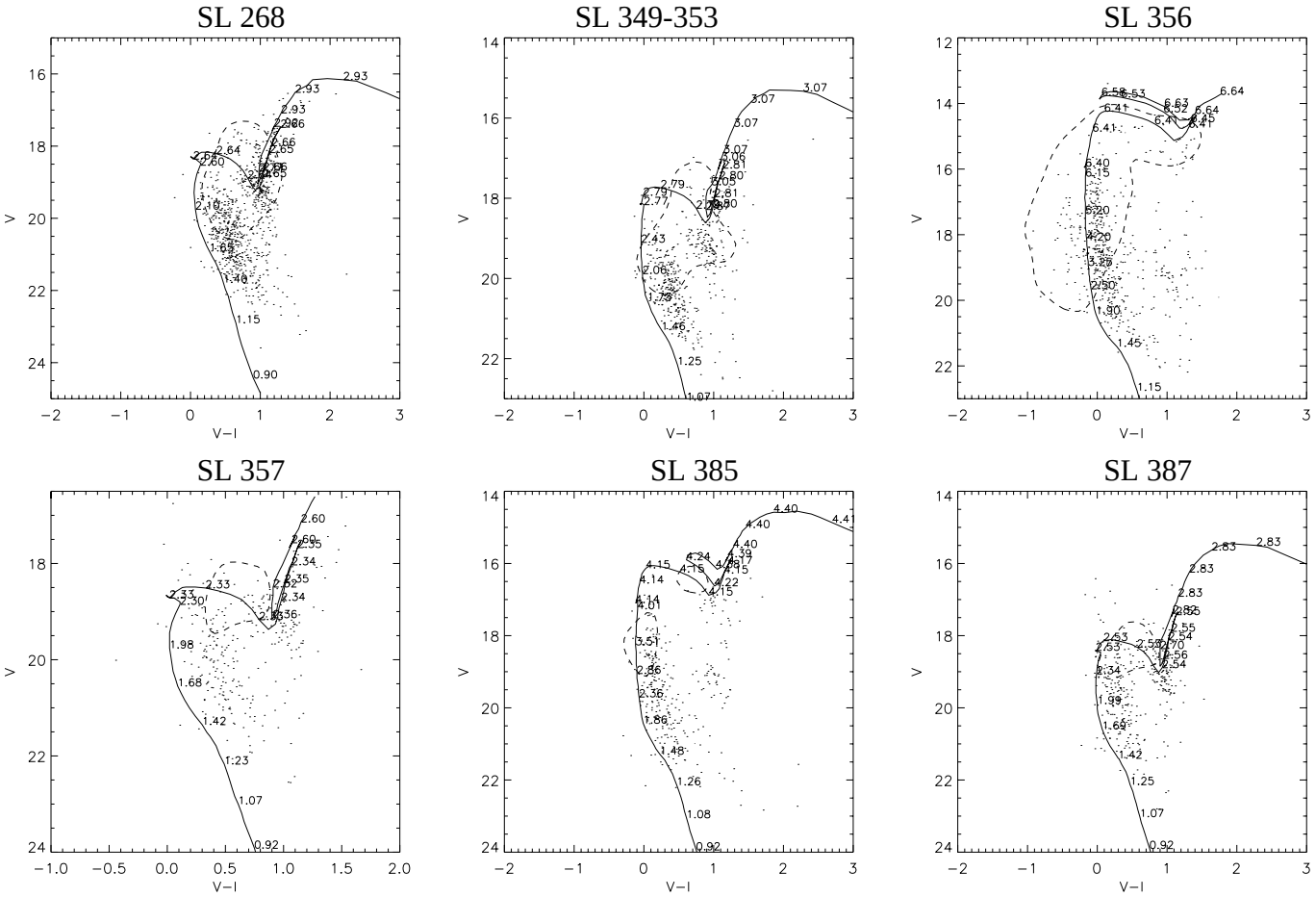

Fig. 3. CMDs of the stars towards the clusters. The dashed line is the mask to select the stars. As we already said, the similarity of the two CMDs in the case of SL 349 and SL 353 makes it impossible to find a reliable area in the CMS to separate the two clusters. Isochrones of the appropriate age are plotted (see Table 1 and for more details Vallenari et al.1998). Stellar masses along the isochrones (in $M_{\odot}$) are also indicated.

The threshold is chosen as a compromise between the highest S/N and star-counts sufficiently high to prevent poissonian noise fluctuation which would decrease the final spatial resolution after the wavelet reconstruction: the higher the S/N threshold, the better the separation between the field stars and the cluster members, and between the clusters themselves with the constraint to be above 3σ poissonian star-counts noise.

On the CMD-selected star counts map we fit a background map following G95 by masking the cluster (from one cluster radius $r_{\rm cl}$ to $2 \times r_{\rm cl}$) and using a blanking value inside, equal to the mean between 1.5 and $2.5 \times r_{\rm cl}$ to get a smooth background: we fit a low-order bivariate polynamial surface, mainly first or second order surface to avoid to erase some local variation by higher order polynomials (see G95). We subtract this background from the CMD-selected map.

On that final density map a Wavelet Transform (WT) is performed, using the so-called "à trous" algorithm (see Bijaoui 1991) which decomposes a 2D array in different planes, each one being a representation of a particular scale. A more complete discussion of the use of WT can be found in Leon et al.(1999). We retain only the planes 3 to 7, removing the highest planes which represent the low scale details. Different tests on the final map have shown (cf. Leon et al.1999) that this resolution can be used at a high confidence level. Typically the map resolution in the cluster region is about $15''$. On Fig. 4 the tidal tail density distribution for each cluster is shown.

3.2. Tidal tail mass

We perform star-counts in the tail by masking the cluster itself, first using the radius of the cluster $r_{\rm cl}$ given by Bica et al.(1996) and shown in Table 1, and second, defining a radius $2 \times r_{\rm cl}$. Then we mask the star-count from the density above a threshold, which is chosen as the lowest level on the Fig. 4. An example of mask, for the object SL 387, is shown on Fig. 5.

To derive the stellar mass released in the tail we estimate the ratio of stars in the CMD mask used to select the stars relatively to the total number of stars. The stellar mass range in the clusters are derived from the isochrone fitting of the cluster CMDs made by Vallenari et al.(1998).

In Fig. 3 the CMDs and the appropriate isochrones are shown for each cluster, together with the involved stellar masses. We define for each object $M_{\rm min}$ and $M_{\rm max}$ as the minimum and maximum stellar masses respectively, in selected mask of the

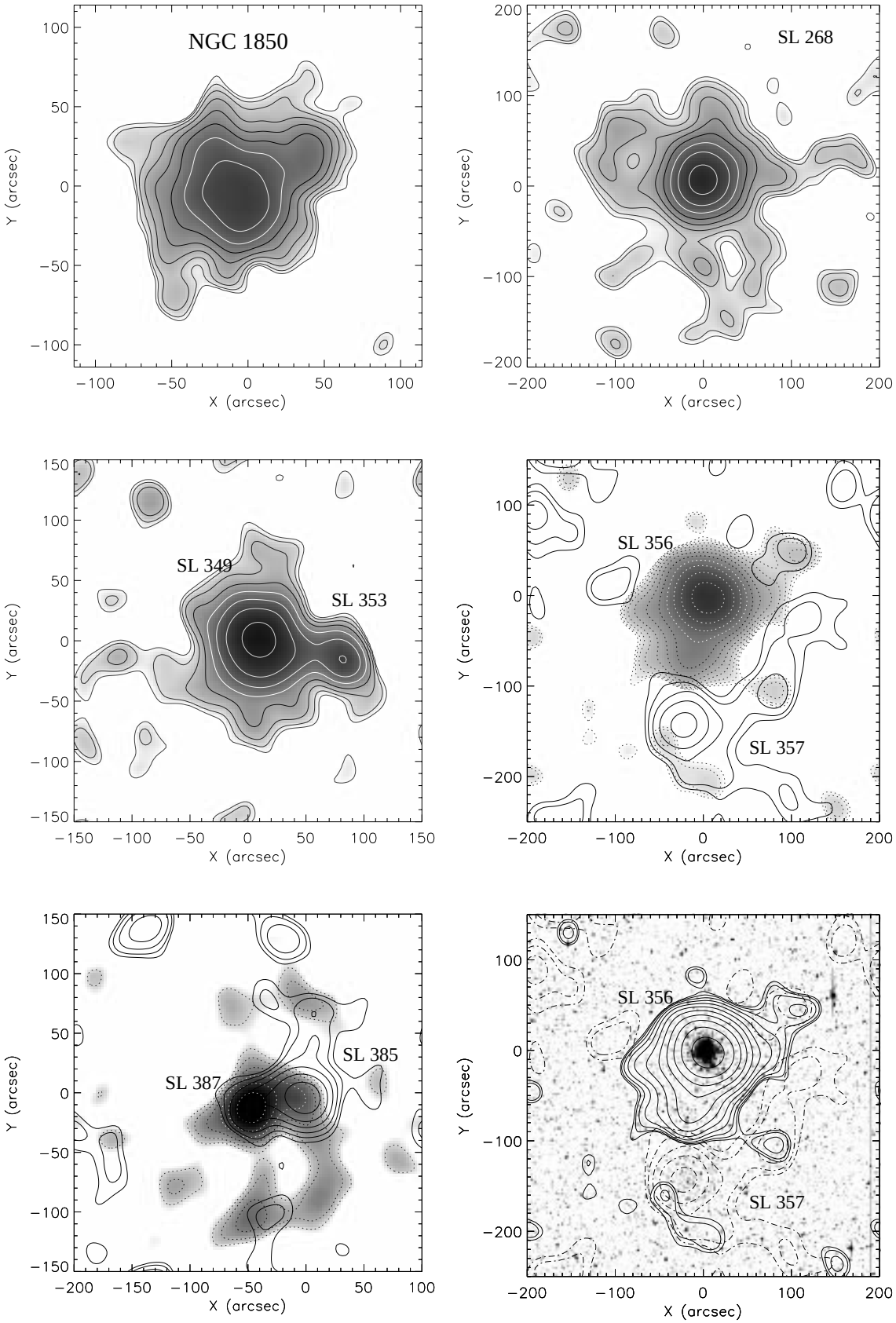

Fig. 4. Surface density (Log) of the star clusters. For SL 356-SL 357 and SL 385-SL 387 contours stand for one of the components. In addition, we present in the lower-right panel the optical image of the pair SL 356-SL 357 overlaid by the same contours.

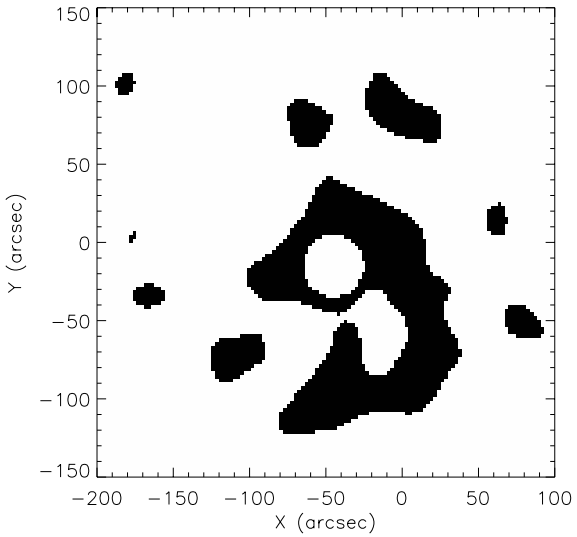

Fig. 5. Example of mask on the tail of SL 387 used to count the stars selected from the CMD mask. We mask as well the cluster using a radius from Bica et al.(1996).

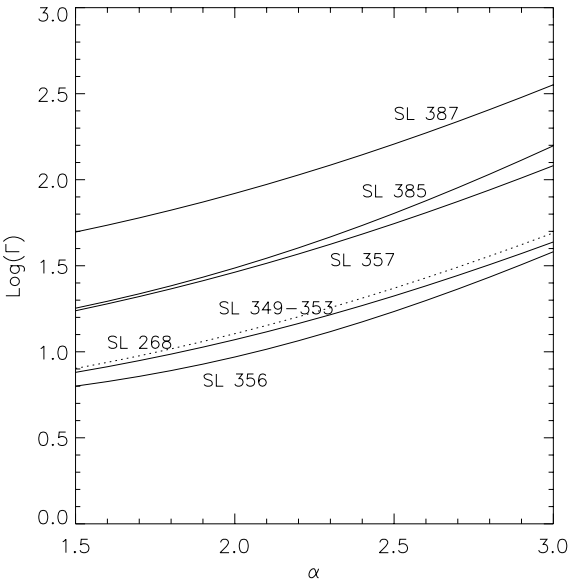

Fig. 6. Gamma estimation for the studied clusters *vs.* the slope of the mass function, relative to the parameters of the CMD mask used to select the stars. The isolated cluster SL 268 is in dotted line. The data referring to NGC 1850 are not shown (see text for details).

CMD. We make use of a Salpeter law for the initial mass function (IMF):

$$\Phi(m) = Km^{-\alpha}, \quad m_{\rm low} < m < m_{\rm up} \tag{1}$$

where α is the slope, $m_{\rm low} = 0.2{\rm M}_{\odot}$ and $m_{\rm up}$ are the lowest and highest stellar masses respectively, in the whole cluster. K is a normalization constant.

Finally, the conversion factor Γ between the total mass in the tail and the number of stars in the selected region (mask) of the cluster CMD is given by the formula:

$$\Gamma = M_{\rm tail}/N_{\rm mask} = \frac{1-\alpha}{2-\alpha}\,\frac{m_{\rm up}^{2-\alpha} - m_{\rm low}^{2-\alpha}}{M_{\rm max}^{1-\alpha} - M_{\rm min}^{1-\alpha}} \tag{2}$$

Γ is critically depending on the adopted value of $m_{\rm low}$ and on the IMF slope α (see Scalo 1997 for an exhaustive discussion of the topic). Table 2 gives the parameters used to compute the tidal tail mass in each object. In the whole mass range a Salpeter slope ($\alpha = 2.35$) is adopted.

Nevertheless, we must point out that several effects might influence our results:

(i) The clusters we have analyzed are affected by a severe crowding. This can result in a underestimate of the stellar density. This effect becomes relevant mainly at fainter magnitudes and towards the center of the cluster. However, our star-counts are based on the brightest part of the CMD ($V > 20$), less affected by the crowding. From the usual experiments with artificial stars, we estimate that the incompleteness correction, defined as the ratio of the number of recovered stars to the total, is higher than 75–80% for magnitudes brighter than $V = 20$, but becomes higher than 95% for $V < 19$.

(ii) The Γ conversion factor between the star-counts in the tail and the total mass of the tail is the most important source of uncertainty, changing of an order of magnitude when the slope ranges from 1.5 to 3.0. Fig. 6 shows the variation of Γ in the observed clusters at changing IMF slope. NGC 1850 is not included, since the small field of view has prevented any reliable determination. The result of Fig. 6 reflects the fact that the initial mass function slope in the LMC clusters is poorly constrained by the observations. Additional difficulties arise when mass segregation is present, as it is found in the young LMC clusters SL 666 and NGC 2098 (Kontizas et al.1998). The Γ factor is as well dependent on the minimum mass $M_{\rm min}$ selected by the CMD-masking. The Γ estimate is less influenced by the value of the upper mass $M_{\rm up}$.

(iii) To define the selected cluster region, we make use of the diameters from Bica et al.(1996) which are not the tidal radii $r_{\rm t}$. However, deriving the tidal radius of both the components of a pair is quite difficult, because of the mutual interaction between the clusters. In the case of SL 357, choosing a radius twice as

Table 2. $N_{\rm tail}$ is the star count from the CMD mask in the tails, in parenthesis we give the same estimate masking the cluster with a radius twice as larger.

Cluster	$N_{\rm tail}$	$M_{\rm min}$ ($\rm M_{\odot}$)	$M_{\rm max}$ ($\rm M_{\odot}$)	$m_{\rm up}$ ($\rm M_{\odot}$)	$M^{\ddagger}_{\rm tail}/M^{\S}_{\rm cl}$ ($10^3\rm M_{\odot}$)
SL 268	450(290)	1.80	2.90	2.93	8.6 / 17
SL 349	450(190)†	1.73	2.90	3.10	7.8
SL 353	450(190)†	1.73	2.90	3.10	7.8
SL 356	130 (50)	1.90	6.64	6.64	1.8 / 26
SL 357	610(540)	2.10	2.58	2.61	27.4
SL 385	130(100)	2.85	4.00	4.42	6.5
SL 387	230(180)	2.35	2.54	2.83	29.9

† no distinction between the two clusters SL 349 and SL 353.
‡ $M_{\rm tail}$ is the mass in the tails given for a Salpeter slope (2.35).
§ $M_{\rm cl}$ is the estimated total mass of the cluster.

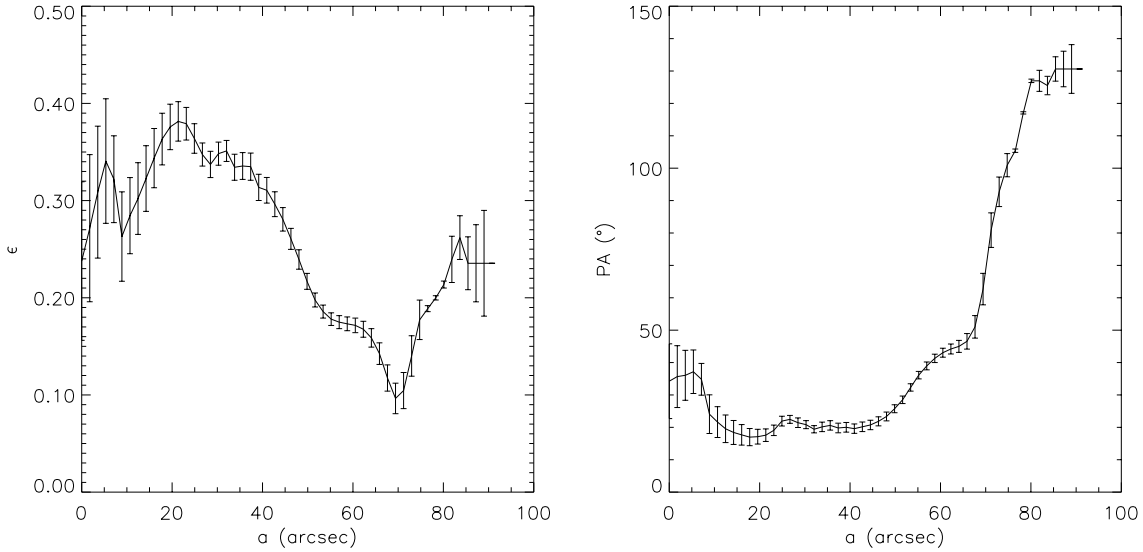

Fig. 7. Ellipticity ϵ (*left*) and position angle PA (*right*) *vs.* semi-major axis for NGC 1850.

large results in a mass determination 10% lower. Nevertheless the correction becomes more relevant for clusters having higher density as shown in Table 2.
(iv) Pollution from overdensities not related to the cluster cannot be avoided, as in the case of SL 385 with an overdensity in the north-east corner which is the cluster NGC 1926 ≡ SL 403 (see Fig. 4). However, because of high S/N on the CMD mask, this effect is not expected to strongly bias the results.

Finally, when all these effects are taken into account, we can estimate that the tidal mass indicated in Table 2 is likely to be an upper limit to the real mass loss of the clusters.

4. Discussion

In this section, we discuss the results for each cluster pair separately. Hints about the most probable formation scenario of binary clusters are given.

4.1. NGC 1850

NGC 1850 (≡ SL 261) is a massive cluster which could be part of a binary or triple system (see Fischer et al.1993; Vallenari et al. 1994). As already stated in previous sections, we did not perform star-counts in the outermost halo of the cluster, because of the small field of view. We have performed an ellipticity and position angle analysis using `ellipse` IRAF task that we show in Fig. 7 to separate the core/halo structure. The surface density presents an elongated shape (see Fig. 4) with an ellipticity $\epsilon \sim 0.25$ oriented in the direction NW-SE (PA$\sim$130°).

The NW tail can be seen on the optical image as a concentration of stars. Contrary to the other clusters, showing quite regular isophotes in the inner regions, NGC 1850 exhibits very disturbed isophotes even at small radii which could be interpreted as due to the interaction with the other very close components. The core structure is elongated perpendicularly to the outer isophote (PA $\sim 20°$). NGC 1850 is the only case in our sample exhibiting a high core ellipticity which could be attributed to strong tidal interactions in a triple system.

Fischer et al.(1993) noted the presence of two diffuse clusters inside a radius of 6′ from NGC 1850 center. We tentatively interpret this structure as due to stars stripped by the cluster by gravitational "harassment" in this very crowded region at the border of the LMC bar.

From a (V, $B-V$) CMD, Vallenari et al.(1994) found 3 components (called A, B, C) located inside about 1′ from the cluster center. They estimated the ages of components A and C to be about 6×10^7 years, whereas the youngest component, B, has an age of 8×10^6 years. The age difference between the components is marginally consistent with the time scale expected on the basis of the model by Fujimoto & Kumai (1997).

4.2. SL 268

SL 268 is an isolated cluster we have used to calibrate the tidal effect of the LMC bar field on the clusters. Clearly the interaction with the gravitational tidal field of the LMC has strong effect on the cluster evolution. The NS tidal extension is 60 pc large. In the southern part of it, the low density region is an artefact due to the presence of a bright star. The tidal tail protruding towards NE accounts for a large part of the $8.6 \times 10^3 M_\odot$ present in the tails.

A fit of the surface density in the halo of the cluster is performed, using a power law function. The surface density, as shown in Fig. 8, is decreasing as $r^{-\gamma}$ with γ=2.27. This is consistent with the results by Elson et al.(1987), hereafter EFF, who found for a sample of LMC clusters typical values of γ ranging from 2.2 to 3.2. However, we point out that, due to the tidal distortion of the isophotal contours, this one-dimensional profile is not a good representation of the spatial distribution which is far from being uniform with the position angle. This profile, as found by EFF, means that as much as 50% of the total mass of the cluster could be in an unbound halo. We can estimate the

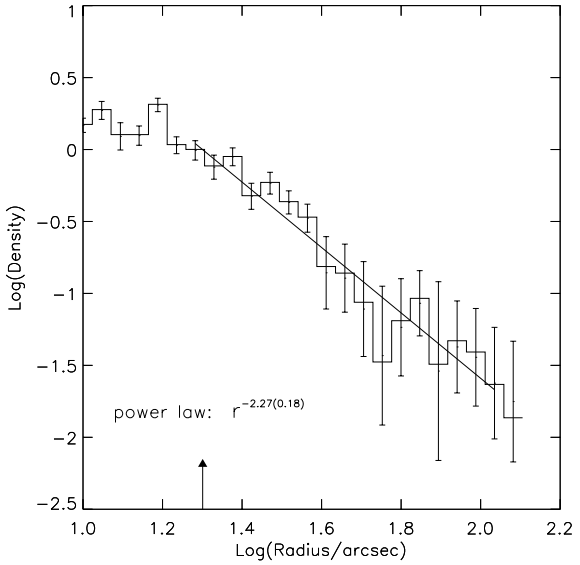

Fig. 8. SL 268: surface density of stars selected from the CMD mask. The arrow is at the position of the cluster masked to count the halo and evaporated stars. The surface density is fitted by a power-law in the outskirts with a slope of 2.27(± 0.18). To have an estimation of the surface density mass, the values have to be multiplied by the Γ correction.

mass of SL 268 to be about $1.7 \times 10^4 M_\odot$, following the procedure outlined by EFF and taking the value of NGC 2004 in EFF which has a slope similar to the one of SL 268. We remind that in the Galactic globular clusters the tidal tail mass represents only a few percents of the cluster mass (Combes et al.1999; Leon et al.1999) where the tidal stripping by the Galactic potential well is much stronger and efficient.

4.3. Pair SL 349-SL 353

Because of their very similar CMDs, SL 349 and SL 353 ($\equiv$ Hodge 1) cannot be separated, as discussed in previous sections. For this reason, no density profiles are presented. The total tidal tail mass of the pair is $7.8 \times 10^3 M_\odot$. The tidal extension in the NS direction associated with SL 349 (see Fig. 4) is similar to the one of SL 268 and could be interpreted as due only to the LMC tidal field. The tail going towards the east along the southern side of SL 349 is difficult to be explained in that way. Even if a projection effect cannot be ruled out totally, it is tempting to associate it to the presence of SL 353. A similar effect is noticed in the case of SL 357 (see following section).

According to Bhatia (1990), the survival time of binary system immersed in the LMC tidal field is at maximum of the order of $\sim 4 \times 10^7$ yr. This pair, with an age of 5×10^8 yr, is an example of old surviving binary pair. We refer to this as the "overmerging" problem. This long lifetime might be explained by the scenario proposed by Bica et al.(1992): star clusters form in groups (Star Cluster Groups, SCGs) inside Giant Molecular Clouds (GMCs) with a high star formation efficiency. The burst of cluster formations can be enhanced during a longer period than the one needed to produce a single cluster ($\sim 10^7$ years).

Table 3. SCG memberships relative to the cluster observed (#1). The criteria are the following: projected distance to the cluster less than 0.25° and with SWB type different at most by one unity (from Bica et al.1996).

#1	#2	#3	#4	#5	#6	#7
SL349	SL353	SL379	SL390			
SL356	SL357	SL344	SL358	SL361	S Dor	SL373
SL385	SL387	SL358	SL403	SL418		

This is in agreement with Efremov & Elmegreen (1998) who find that the star formation process is hierarchical in time and space: small regions are expected to form stars on short time scale (less than 10^6 years), whereas large regions form stars over longer periods ($\geq 3 \times 10^7$ yr).

If the clusters are formed as a part of SGC, it is not necessary that the pair SL 349-SL 353 was formed in a bound binary system, but tidal capture at later time could have been at work. In fact, inside such a high density SCG the rate of encounters must be higher than for isolated clusters (see next section).

At the light of these works, we suggest that SL 349 and SL 353 are part of a SCG. Using the integrated photometry of LMC clusters by Bica et al.(1996), we tentatively identify the objects forming this SCG. We present the list in Table 3. The clusters are selected with the following criteria: cluster distance to "central" (arbitrary) cluster less than 0.25° and a SWB type (defined by Searle et al. 1980) differing at most of one unity from the SWB type of the central cluster.

The star formation in the GMCs could have been triggered by interaction between LMC and SMC. Elmegreen & Efremov (1997) have proposed that large-scale shocks can explain the formation of star clusters in interacting galaxies. It is tempting to associate the younger SCGs to the interaction of the LMC with the SMC which would have strongly enhanced the cluster formation a few 10^8 years ago.

4.4. Pair SL 356-SL 357

SL 356-SL 357 is a puzzling pair because of the large age difference between the two components, respectively 70 Myr for SL 356 and 600 Myr for SL 357. This age difference allows us to disentangle both the components on the basis of the CMD properties. SL 356 ($\equiv$ NGC 1903) does not exhibit extended structures (see Fig. 4). A southern tail is actually connected with the secondary component, already found by Vallenari et al.(1998). In comparison with the other clusters (see Table 2), it has no massive halo, which is explained with its steep surface density profile in the outskirts (Fig. 9): a power law of slope $\gamma = 3.44$ is consistent with the data.

Following EFF method, we derive for SL 356 the total mass of $2.6 \times 10^4 M_\odot$. SL 357 appears optically much weaker and more diffuse than SL 356 (see Fig. 4). This object presents a very large tail which is obviously due to its interaction with SL 356, as predicted by numerical simulations (de Oliveira et al. 1998).

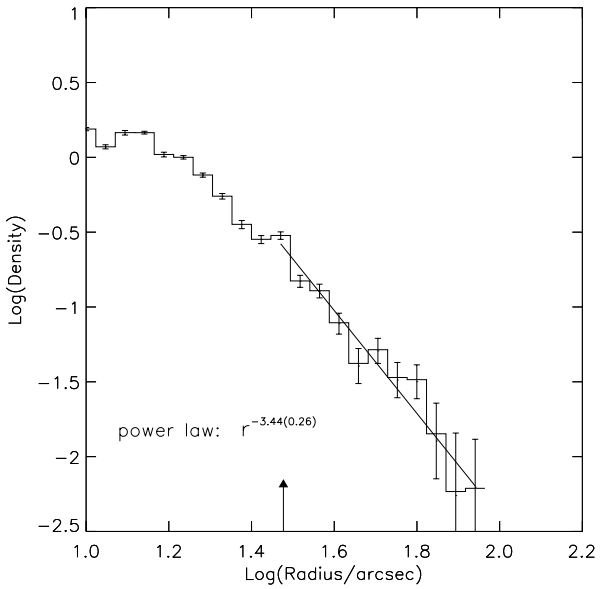

Fig. 9. SL 356: surface density of stars selected from the CMD mask. The arrow is at the position of the cluster masked to perform tidal tail star-counting. The surface density is fitted by a power-law in the outskirts with a slope of -3.44 (± 0.26). To have an estimation of the surface density mass, the values have to be multiplied by the Γ correction.

We point out that the age difference between the two components is too large to be consistent with the Fujimoto & Kumai (1997) model of binary cluster formation. Invoking a SCG scenario for SL 356-SL 357 (see Table 3), the formation of this pair by tidal capture becomes more probable, because of an enhanced geometric cross section for the rate of encounters per cluster. Following Lee et al.(1995) we estimate a rate of encounters $\frac{\mathrm{d}N}{\mathrm{d}t} \sim 10^8$ years for a cluster crossing a SCG, which is compatible with the age of SL 357 and with the large separation of the two clusters (40 parsecs). The response to the interaction is different for the two clusters: it is plausible that the concentration of SL 356 was greater than the one of SL 357, as suggested by the steep outer surface density.

We have to point out that the mass of SL 356, estimated from its low halo mass could be underestimated, while the estimation mass of the tail of SL 357 is likely overestimated, thus an unequal mass system cannot be ruled out as suggested by the Fig. 4 of de Oliveira et al.(1998) which is is very similar to this system.

4.5. Pair SL 385-SL 387

These two clusters present completely different spatial distribution in the halo: SL 387 exhibits tidal tails typical of stellar systems in interaction (see e.g., Hibbard & van Gorkom 1996 for interacting galaxies; de Oliveira et al. 1998 for binary clusters), with a mass loss 5 times larger than SL 385. SL 385 presents a modest extension closely resembling to SL 268, and due – at least partially – to the gravitational tidal field of the LMC. The projected separation (10 pc) between the pair components suggests that they will merge rapidly in $\lesssim 10^7$ years (see Sugimoto & Makino 1989; Bhatia 1990).

From the simulations of Sugimoto & Makino (1989) for two interacting clusters, it appears that the stars lie in the trailing side of the orbiting binary: the orbital spin must be an anti-clockwise orbital path in projection on the sky. As in the case of the pair SL 349-SL 353, SL 385-SL 387 are both older than 10^8 years: the overmerging problem arises once more for such a close binary system.

The SCG formation scenario can represent a convincing explanation for the formation of this pair. The list of clusters tentatively identified as belonging to this SCG together with SL 385 and SL 387 is given in Table 3.

Finally, we point out that due to the small separation of the pair, density profiles cannot be used to derive the total masses of the clusters.

5. Conclusion

We study the tidal tail extensions of 8 star clusters in the LMC bar, using star-counts on the CMDs. Seven of these clusters are suspected to belong to binary or multiple systems, while one (SL 268) is isolated. The presence of tidal tails typical of stellar systems in interaction confirms that all the pairs are physically connected, as already found for other binary clusters by Kontizas et al. (1993): it appears that in their cluster sample, the ages of the binaries are less than a few 10^7 years and a coeval evolution before the merging cannot be ruled out. Nevertheless we point out that their objects are located in a cluster-rich environment which can be related to a Star Cluster Group (SCG).

The isolated cluster SL 268 have about 50% of its mass in its outskirts, as found already for other clusters by EFF. The halo density distribution of this cluster appears to be strongly shaped by the LMC tidal field. The luminosity profiles of SL 268 and SL 356, at large radii, fall off as $r^{-\gamma}$, with γ equal to 2.27 and 3.44 respectively, in good agreement with the values found by EFF.

All the observed pairs are older than the survival time of binary clusters estimated by theoretical models (less than 4×10^7 years, see Bhatia 1990; Sugimoto & Makino 1989). We refer to this as the "overmerging" problem. The star cluster group (SCG) scenario invoking the formation of these clusters as part of a large group during the last interaction with the SMC, can help in solving this problem. We point out that a recent study of binary clusters in the SMC discloses the same "overmerging" problem (Dieball & Grebel 1998). We suggest that this scenario formation in SCG induced by tidal interaction with the SMC is different with the quiescent one in the Milky Way: the binary cluster frequency appears to be much lower, despite the opposite claim of Subramaniam et al.(1995). In the SCGs binary clusters could have formed with a delay compatible with the current age found in the studied pairs. This scenario, as well, could explain the peculiar pair SL 356-SL 357 which would have form from a tidal capture of SL 357 by the more massive cluster SL 356, thanks to a cross section increased in the SCG. We tentatively

give in the memberships of the different SCGs selected from the survey of Bica et al.(1996).

A dynamical study of the SCGs would be of great interest. A more complete identification of SCGs and a dynamical analysis of star clusters embedded in the LMC field will be presented in forthcoming papers.

Acknowledgements. We thank G. Meylan for his helpful remarks and V. Charmandaris for his XIRAF scripts. We also gratefully acknowledge useful comments from the referee M. Kontizas.

References

Bergond G., Leon S., Guibert J., 1999, in prep.
Bhatia R., 1990, PASJ 42, 757
Bhatia R., Hatzidimitriou D., 1988, MNRAS 230, 215
Bhatia R., Read M., Hatzidimitriou D., Tritton S., 1991, A&AS 87, 335
Bica E., Clariá J., Dottori H., 1992, AJ 103, 1859
Bica E., Clariá J., Dottori H, Santos J.F.C., Piatti A.E., 1996, ApJS 102, 57
Bijaoui A., 1991, The wavelet transform. In: Data Analysis Workshop 3, 3
Combes F., Leon S., Meylan. S., 1999, in prep.
Dieball A., Grebel E.K., 1998, Binary clusters in the Magellanic Clouds II: The Small Magellanic Cloud. In: Annual Scientific Meeting of the Astronomische Gesellschaft at Heidelberg, September 14–19, 1998, poster #P72
Efremov Y., Elmegreen B., 1998, MNRAS 299, 588
Elmegreen B., Efremov Y., 1997, ApJ 480, 235
Elson R., Fall M., Freeman K., 1987, ApJ 323, 54 (EFF)
Fischer P., Welch D., Mateo M., 1993, AJ 105, 938
Fujimoto M., Kumai Y., 1997, AJ 113, 249
Goodwin S.P., 1997, MNRAS 286, L39
Grillmair C.J., Freeman K.C., Irwin M., Quinn P.J., 1995, AJ 109, 2553 (G95)
Grondin L., Demers S., Kunkel W., 1992, AJ 103, 1234
Hibbard J., van Gorkom J., 1996, AJ 111, 655
Kontizas E., Kontizas M., Michalitsianos A.G., 1993, A&A 267, 59
Kontizas M., Hatzidimitriou D., Bellas -Velidis I., et al., 1998, A&A 336, 503
Lee S., Schramm D., Grant J., 1995, ApJ 449, 616
Leon S., Meylan G., Combes F., 1999, in prep.
de Oliveira M.R., Dottori H., Bica E., 1998, MNRAS 295, 921
Scalo J., 1997, In: Gilmore G., Howell D. (eds.) The Stellar Initial Mass Function (38th Herstmonceux Conference). ASP Conference Series 142, 201
Searle L., Wilkinson A., Bagnuolo W.G., 1980, ApJ 239, 803
Subramaniam A., Gorti U., Sagar R., Bhatt H.C., 1995, A&A 302, 86
Sugimoto D., Makino J., 1989, PASJ 41, 1117
Vallenari A., Aparicio A., Fagotto F., et al., 1994, A&A 284, 447
Vallenari A., Bettoni D., Chiosi C., 1998, A&A 331, 506